CHAPTER 104

LONGSHORE CURRENT AND TRANSPORT ACROSS NON-SINGULAR EQUILIBRIUM BEACH PROFILES

Kevin R. Bodge¹ (Associate Member, ASCE)

ABSTRACT

The longshore current and longshore sediment transport distributions are described across an equilibrium beach profile comprised of an intersecting planar foreshore and a concave-up profile. Such a profile shape avoids the singularity associated with the infinite-slope at the shoreline described by traditional equilibrium profile forms and allows prediction of beach processes at and above the shoreline. The mathematical expressions which describe the distributions are simplified and can be more readily applied relative to expressions previously presented in the literature. The findings are in general agreement with similar previous analytic studies and indicate that the current and transport maxima are generally located at about the intersection of the planar and concave-up portions of the profile.

INTRODUCTION

Recent analytical solutions and data indicate that the longshore current and transport distributions across non-planar beaches can be markedly different than that predicted for planar beaches (see Sawaragi and Deguchi, 1978; Berek and Dean, 1982; Sternberg et al., 1984, Bodge and Dean, 1987; Fulford, 1987; Kraus, Rosati and Gingerich, 1988; Bodge, in press; among others). Since few natural beaches are planar in profile, the solution of the longshore current and transport distributions across non-planar beaches is relevant to improved understanding and modelling of littoral processes for physically realistic beach profiles.

BACKGROUND

Bruun (1954) and Dean (1977) have suggested that equilibrium beach profiles are described by the form

$$h = a x^{2/3}$$

(1)

¹Senior Engineer, Olsen Associates, Inc., 4438 Herschel Street, Jacksonville, FL 32210.

where h=depth, x=distance offshore, and a is a dimensional coefficient. A disadvantage of the concave-up profile described by this equation is the infinite beach slope at the shoreline (x=0) which leads to (i) a singularity in the description of the longshore current and transport at the shoreline, and (ii) no description of the swash zone. In contrast, most equilibrium profiles in nature are characterized by a relatively planar beachface which extends from the berm to just below the shoreline.

McDougal and Hudspeth (1984) analytically considered the wave-induced set-up and longshore current and transport across beach profiles described by a planar foreshore and an $ax^{2/3}$ -type profile seaward of the foreshore. These authors considered both "stress" and "energetics" longshore transport models after Komar (1977) and Bagnold (1963), respectively:

In the present study, the set-up, longshore current and longshore transport across such a combined planar-foreshore/concave-up profile is analytically described using (1) the longshore current solutions described by Longuet-Higgins (1970) and in part by McDougal and Hudspeth (1984), respectively, across the planar and concave-up portions of the profile; (2) a simplistic assumption that the local wave height is proportional to the local set-up water depth, and (3) a distributed longshore transport model described by Bodge and Dean (1987).

THE NON-SINGULAR EQUILIBRIUM BEACH PROFILE

Consider a beach profile such as shown in Figure 1 with x-axis directed offshore and origin x=0 at the still water shoreline. The profile is composed of two mathematically described segments: (1) a planar foreshore of slope mf, and (2) a concave-up profile of the form $h=ax^{2/3}$, where h is the still-water depth and a is a shape parameter. The profiles intersect at the "match-point" x=xm. The usual origin of the concave-up profile (i.e., at depth h=0) is displaced seaward of the x-axis origin by the distance δ . Specifically,

$$h = \begin{cases} m_{f} x & x \leq x_{m} \\ a(x-\delta)^{2/3} & x \geq x_{m} \end{cases}$$
(1)

Requiring that the bottom depths and slopes are identical at the match-point $\boldsymbol{x}_{\text{M}}$ yields

$$x_{m} = \frac{4}{9} \frac{a^{3}}{m_{f}^{3}}$$
(2)

and

$$\delta = \frac{x_{\rm m}}{3} \tag{3}$$

That is, the location of the match-point can be simply

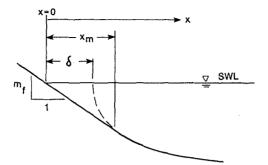


Figure 1: The non-singular equilibrium beach profile.

described by the foreshore slope and the shape factor of the concave-up part of the profile.

WAVE-INDUCED SET-UP

The variation in mean water surface associated with change in onshore radiation stress, or wave-induced set-up \bar{n} , has been shown to be equal to

$$\bar{\eta} = \begin{cases} \nu(h_b - h) - \frac{\kappa^2}{16} h_b & x \leq x_b \\ \frac{-H^2 k}{8 \sinh 2kh} & x \geq x_b \end{cases}$$
(4)

after Longuet-Higgins and Stewart (1964), and Dean and Dalrymple (1984), among others, where h_b and x_b are the still-water depth and location of the wave breakpoint, respectively, H is the local wave height, and k is the wavenumber. Shoreward of the breakpoint, the wave height H is assumed proportional to the total water depth d, where

 $\kappa = H/d$ (5)
and $v = \frac{3\kappa^2}{8 + 3\kappa^2}$ (6)

Across the planar foreshore part of the profile, the slope of the set-up water surface is uniform and equal to $-\nu m_f$. The point of intersection of the set-up water surface and the foreshore, x_s , is

 $x_{s} = \frac{(v - \kappa^{2} / 16) h_{b}}{(v - 1) m_{f}}$ (7)

This location corresponds to the "set-up still water line", or more precisely, the mean water line in the influence of static wave set-up.

The total water depth d across the profile is

$$d = h + \bar{\eta}$$

Combining Eqs. (1), (4), and (8), the total water depth across the non-signular equilibrium profile is

$$d = \begin{cases} (1-\nu) m_{f} x + (\nu - \frac{\kappa^{2}}{16}) h_{b} & x_{s} \le x \le x_{m} \\ \\ (1-\nu) a (x-\delta)^{2/3} + (\nu - \frac{\kappa^{2}}{16}) h_{b} & x \ge x_{m} \end{cases}$$
(9)

For purposes of notation, observe that the set-up water surface slope across the planar foreshore part of the profile is

$$s_{f} = (1-v) m_{f}$$
 (10)

McDougal and Hudspeth (1981, 1984) showed that the total water depth across the concave-up $h{=}ax^{2/3}$ profile can be well-approximated by the form

$$d = \tilde{a} x^{1/2}$$
(11)

This expression models the set-up water surface well except as x approaches 0 (since d does not go to zero as x+0). However, the poorer fit near x=0 is essentially inconsequential in the present case if the <u>exact</u> form of the set-up water surface is used across the planar foreshore part of the profile; i.e., in the region x=0. Accordingly, the following expressions are adopted for the total water depth:

$$d = \begin{cases} s_{f} x + (v - \frac{\kappa^{2}}{16}) h_{b} & x_{s} \leq x \leq x_{m} \\ \hat{a} (x - \hat{\delta})^{1/2} & x \geq x_{m} \end{cases}$$
(12)

Requiring continuity of total water depth and water surface slope at the matchpoint \boldsymbol{x}_m yields

$$\hat{a} = s_{f} \sqrt{2(x_{m} - x_{s})}$$
 (13a)
 $\hat{a} = \frac{1}{2} (x_{m} - x_{s})$

$$\delta = \frac{1}{2} \left(x_{\rm m}^{+} x_{\rm s}^{-} \right) \tag{13b}$$

Non-dimensionalizing all length scales by the distance to the breakpoint \mathbf{x}_{b} yields

$$D = \begin{cases} s_{f} X + (v - \frac{\kappa^{2}}{16}) s_{b} & X_{s} \leq X \leq X_{m} \\ \hat{A} (X - \hat{\Delta})^{1/2} & X \geq X_{m} \end{cases}$$
(14)

$$\hat{A} = s_{f} \sqrt{2(x_{m} - x_{s})}$$
 (15a)

(8)

$$\hat{\Delta} = \frac{1}{2} \left(X_{\rm m} + X_{\rm s} \right) \tag{15b}$$

where upper-case denotes non-dimensional terms such as

 $X = x / x_{b}$ (16)

and where the term sb has been introduced as

$$s_{b} = h_{b} / x_{b}$$
(17)

LONGSHORE CURRENT

In dimensional form, wave-induced longshore current can be described through the depth- and time-averaged equation of motion in the alongshore direction (Bowen, 1969; Longuet-Higgins 1970),

$$\frac{\partial}{\partial x} S_{xy} + \tau_{by} + \frac{\partial}{\partial x} (\mu_e \ d \ \frac{\partial}{\partial x} v \) = 0$$
(18)

where S_{xy} is the onshore-directed flux of the alongshore component of momentum, τ_{by} is the alongshore component of bottom stress, v is the depth- and time-averaged longshore current, and μ_e is the turbulent eddy viscosity. Following the classical approximations of Longuet-Higgins (1970) and others,

$$\tau_{\rm bv} = -\frac{\kappa}{\pi} C_{\rm f} \rho \sqrt{\rm gd} \quad v \tag{19}$$

where C_{f} is an empirically determined friction factor of order 0.01. The turbulent viscosity is assumed to vary linearly with distance offshore

$$\mu_{o} = N \rho x \sqrt{gd}$$
(20)

where N is a numerical constant.

<u>Non-dimensionalizing</u> all length-scales by the breaker distance x_b and velocity by the classical Longuet-Higgins solution of longshore current at the breaker line with no mixing, i.e.,

$$v_{o} = \frac{5}{16} \frac{\kappa \pi}{C_{f}} \sin \theta_{b} \sqrt{gd_{b}} s_{b}$$
(21)

where θ is the wave angle and the "b" subscript refers to breaking conditions, the alongshore equation of motion (Eq. 18) becomes

$$\frac{N}{\kappa c_{f}} \frac{\pi}{\partial X} (XD^{3/2} \frac{\partial V}{\partial X}) - D^{1/2}V = -D^{3/2} \frac{\partial D}{\partial X} \frac{1}{s_{b}^{Z}}$$
(22)

where upper-case denotes non-dimensional terms once again such as

$$V = v/v_o$$
 and $X = x/x_b$ (23)

To determine the longshore current, Eq. (22) must be solved across each of three regions across the nonsingular equilibrium profile: (i) the planar foreshore, (ii) the concave-up segment landward of the breakpoint, and (iii) the concave-up segment seaward of the breakpoint. Both the magnitude and gradient of the velocity must be matched between each region. McDougal and Hudspeth (1984) demonstrated these solutions but the resultant expressions are somewhat cumbersome and tedious to apply.

In the present study, Eq. (22) is solved for the longshore current across each of the three regions; both the magnitude and gradient are matched at the planar/ concave-up matchpoint x_m but only the magnitude is matched at the breakpoint x_b . The resulting discontinuity in the velocity gradient at the breakpoint is small for the physically-typical case where x_m is small compared to x_b (i.e., where the toe of the foreshore is located close to shore relative to the breakpoint).

Incorporating the non-dimensional expressions for total water depth D (Eq. 19) to Eq. (22), and solving for velocity subject to the above-described matching conditions, the non-dimensional longshore current is given by

$$v = \begin{cases} A_{1} (X-X_{s})^{P_{1}} + (\frac{s_{f}}{s_{b}})^{2} \frac{1}{1-\frac{5}{2}P} (X-X_{s}) & X_{s} \le X \le X_{m} \\ C_{1} [\frac{\cosh(\lambda \tilde{X}^{1/4})}{\lambda \tilde{X}^{1/2}} - \frac{\sinh(\lambda \tilde{X}^{1/4})}{\lambda^{2} \tilde{X}^{3/4}}] + \frac{\hat{A}^{2}}{2s_{b}^{2}} & X_{m} \le X \le 1 \end{cases} (24) \\ C_{2} [\frac{1}{\tilde{X}^{1/2}} + \frac{1}{\lambda \tilde{X}^{3/4}}] \exp(-\lambda \tilde{X}^{1/4}) & X \ge 1 \end{cases}$$

where

$$P_1 = -\frac{3}{4} + \left(\frac{9}{16} + \frac{1}{P}\right)^{1/2}$$
(25)

$$P = \frac{N \pi s_f}{\kappa c_f}; P \neq 2/5$$
(26)

$$\lambda = 4/\sqrt{P_2}$$
(27)

$$P_{2} = \frac{N \pi \hat{A}}{C_{f}} = P \sqrt{2(X_{m} - X_{s})}$$
(28)

$$\widetilde{\mathbf{X}} = (\mathbf{X} - \widehat{\boldsymbol{\Delta}}) \tag{29}$$

The coefficients are given by

$$A_{1} = (X_{m} - X_{s})^{-p_{1}} [c_{1} \phi - \alpha (X_{m} - X_{s}) + \frac{A^{2}}{2s_{b}^{2}}]$$
(30)

^ 0

$$C_{1} = -\frac{\hat{A}^{2}}{2s_{b}^{2}} (3Q + \lambda Q^{2} + \frac{3}{\lambda}) \exp(-\lambda Q)$$
(31)

$$C_{2} = \frac{\hat{A}^{2}}{2s_{h}^{2}} \left[-\frac{3Q}{\lambda} \cosh \lambda Q + (Q^{2} + \frac{3}{\lambda^{2}}) \sinh \lambda Q \right]$$
(32)

and where

$$\alpha = \left(\frac{s_{f}}{s_{b}}\right)^{2} \frac{1}{1 - \frac{5}{2}P} ; P \neq 2/5$$
(33)

$$\Phi = \frac{1}{\lambda R^2} \cosh \lambda R - \frac{1}{\lambda^2 R^3} \sinh \lambda R$$
(34)

$$R = (X_{m} - \hat{\Delta})^{1/4}$$
(35)

$$q = (1 - \hat{\Delta})^{1/4}$$
 (36)

Application of Eqs. (24) through (36) can be cumbersome. However, each of the terms in Eq. (24) which describe the longshore current can be expressed solely as a function of the non-dimensional matchpoint location X_m and the mixing parameter P. Recall that X_m is simply described by

$$X_{m} = X_{m} / X_{b}$$
(37)

where

$$x_{m} = \frac{4}{9} \left(\frac{a}{m_{f}}\right)^{3}$$
 (38)

and

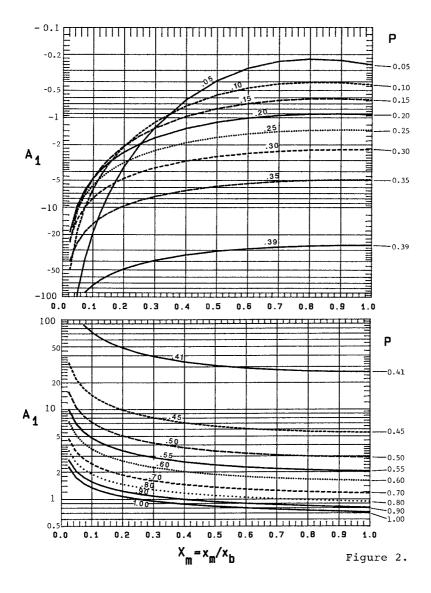
$$x_{b} = \left(\frac{H_{b}}{\kappa a}\right)^{3/2} + \frac{4}{27} \left(\frac{a}{m_{f}}\right)^{3}$$
(39)

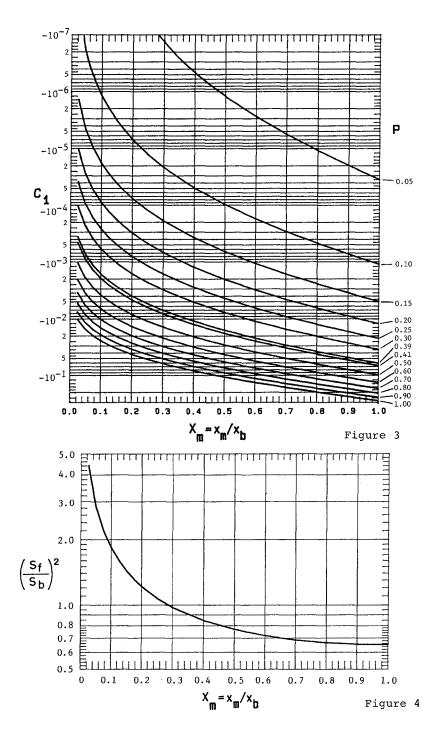
Hence, the non-dimensional longshore current profile can be readily calculated from the (i) breaking wave height H_b , (ii) breaker index κ , (iii) concave-up beach shape parameter a (commonly denoted by "A" in the literature), (iv) foreshore slope m_f , and (v) selection of a mixing parameter P, where P $\neq 0.4$.

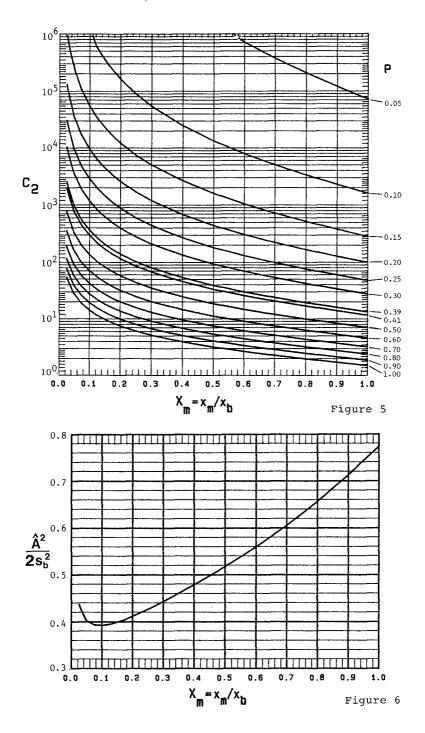
Figures 2 through 9 depict each of the terms necessary to evaluate the longshore current distribution from Eq. (24) for a breaker index $\mathcal{K} = 0.8$, for various chosen values of the mixing parameter P and for calculated values of the non-dimensional planar-foreshore/concave-up matchpoint location $X_{\rm m}$.

Figure 10 illustrates the non-dimensional longshore current across the non-singular equilibrium beach profile for various locations of the profile matchpoint X_m . Note that the current maxima approximately corresponds to the location of the profile matchpoint.

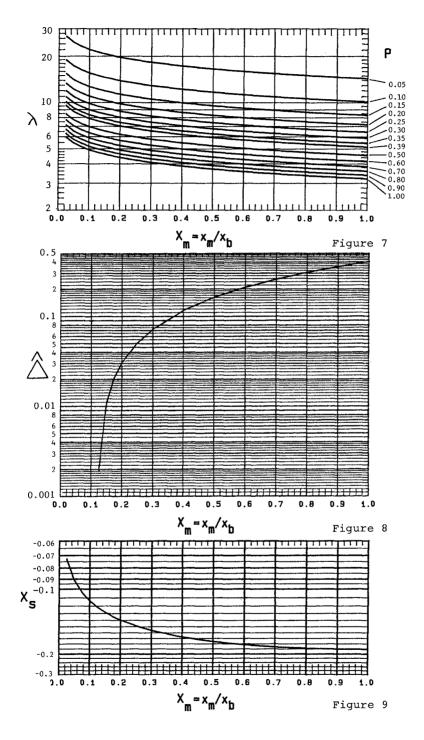
Figure 11 illustrates longshore current distributions observed across beaches with non-singular equilibrium shaped profiles -- compared to the distributions predicted for each case by Eq. (24) for several values of the mixing parameter. The first five cases represent dye observations from a moveable-bed laboratory model for five different breaking/surf conditions; the last case is from current meter data collected at Duck, N.C., (Bodge and Dean, 1987). The agreement is fairly good, although the longshore current distributions observed in the laboratory appear displaced landward by about 2/10'ths of a surf zone width relative to the predicted distributions.







1405



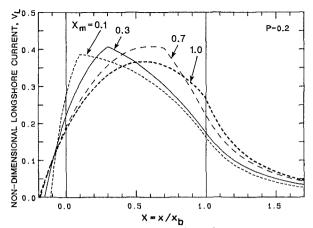


Figure 10: Longshore current predicted across a non-singular equilibrium profile for various profile matchpoints.

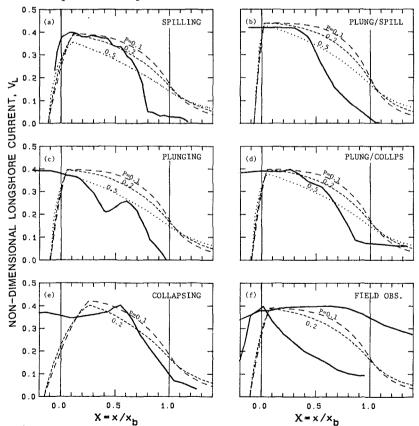


Figure 11: Observed (bold) and predicted (dashed) longshore current distribution across non-planar beaches.

LONGSHORE SEDIMENT TRANSPORT

Bodge and Dean (1987) presented a distributed longshore transport model based upon results of short-term impoundment of longshore sediment transport across rapidly-deployed, low-profile groins in the field and laboratory environments. Their expression suggests that sediment is mobilized in proportion to the rate of local wave energy dissipation per unit surf zone volume and is transported alongshore by local longshore current; viz.,

 $q_{\ell}(x) = k_{\ell} \frac{1}{h} \frac{\partial}{\partial x} (e c_g) v$ (40)

where $q_{\ell}(x)$ is the local longshore sediment transport rate per unit offshore distance, k_{ℓ} is a dimensional coefficient of proportionality, and ec_{g} is the local wave energy flux.

Again assuming that local wave height is proportional to the local water depth, and non-dimensionalizing lengths by the breaker distance and velocities by the planar-beach no-mixing longshore current at the breakpoint, Eq. (40) becomes

$$Q_{\ell} = D^{1/2} s_{b}^{-3/2} V \frac{dD}{dX}$$
 (41)

where Q_{ℓ} is the local (not total) longshore transport rate per unit distance offshore normalized by the local rate at the breakpoint; i.e.,

$$q_{\ell} = q_{\ell} / q_{\ell b}$$
 (42)

where

$$A_{\ell b} = k_{\ell} \frac{5}{16} \rho g^{3/2} \kappa^2 d_b^{1/2} v_o s_b$$
(43)

Equation (41) can be evaluated to yield the longshore sediment transport distribution across the surf zone (landward to the location of the set-up still water line x_S) via Eq. (24) for the longshore current and Eq. (14) for the total water depth. Figure 12 illustrates the transport distributions for various locations of the profile matchpoint X_m . Note that the maxima closely corresponds to the location of the profile matchpoint.

Figure 13 compares the longshore transport distributions across a non-singular equilibrium profile as predicted by the "energetics" model (Bagnold, 1963), the "stress" model (Komar, 1977), and the present model (Bodge and Dean, 1987).

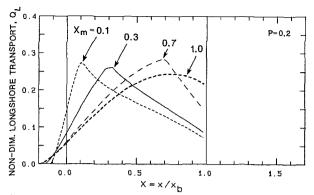


Figure 12: Longshore transport across a non-singular equilibrium profilc for various profile matchpoint locations.

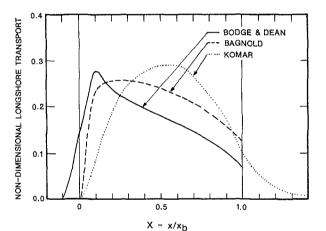


Figure 13: Comparison of longshore transport distribution models evaluated for a non-singular equilibrium profile with matchpoint $X_m=0.1$ and mixing parameter P=0.1.

SUMMARY AND CONCLUSIONS

The non-singular equilibrium beach profile consists of a planar foreshore "matched" to a concave-up profile across the surf zone. The longshore current and sediment transport distributions across such a profile can be readily developed through knowledge of the foreshore slope, concave-up profile shape parameter, breaker height, and selection of a Longuet-Higgins type mixing parameter. The current and transport maxima are predicted at or about the location of the planar-foreshore/concave-up profile matchpoint. Since this point is typically located fairly close to shore relative to the breakpoint, this suggests that the peak current and transport are more closely located to shore than to the breakpoint. This result agrees with similar solutions for non-planar beaches, such as McDougal and Hudspeth (1981, 1984), but is in contrast to classical predictions for planar beaches -- where current and transport is predicted as maximum at the outer half of the surf zone and vanishing at the shoreline. Moreover, the results for the non-planar beach, as in the present study, agree more closely with recent field and laboratory observations.

REFERENCES

Bagnold, R.A., 1963. Beach and Nearshore Processes Part I: Mechanics of Marine Sedimentation. <u>In:</u> M.N. Hill (ed.), <u>The</u> <u>Sea: Ideas and Observations, Vol. 3</u>. New York: Interscience, 507-528.

Berek, E.P. and R.G. Dean, 1982. Field Investigation of Longshore Transport Distribution. <u>Proc., 18th Int. Conf. on Coastal</u> <u>Eng.</u>, ASCE, 1620-1639.

Bodge, K.B., in press. A Literature Review of the Distribution of Longshore Sediment Transport Across the Surf Zone. <u>J. Coastal</u> <u>Research</u>.

Bodge, K.B. and R.G. Dean, 1987. Short-Term Impoundment of Longshore Transport. <u>Proc., Coastal Sediments '87</u>, ASCE, 468-483.

Bowen, A.J. The Generation of Longshore Currents on a Plane Beach. J. Marine Research, 27, 206-215.

Bruun, P., 1954. Coast Erosion and Development of Beach Profiles. Beach Erosion Board, Tech. Memo. No. 44, Washington, DC.

Dean, R.G., 1977. Equilibrium Beach Profiles: U.S. Atlantic and Gulf Coasts. Ocean Eng. Rpt. No. 12, Dept. of Civil Eng., Univ. of Delaware, Newark, DE; 45 pp.

Fulford, E.T., 1987. Distribution of Sediment Transport Across the Surf Zone. <u>Proc., Coastal Sediments '87</u>, ASCE, 452-467.

Komar, P.D., 1977. Beach Sand Transport: Distribution and Total Drift. <u>J. Waterway, Port, Coastal and Ocean Eng.</u>, ASCE, 103, WW2, 225-239.

Kraus, N.C., Rosati, J.D. and K.J. Gingerich, 1988. Longshore Sediment Transport in the Surf Zone. <u>Proc., 21st Conf. on</u> <u>Coastal Eng.</u>, ASCE.

Longuet-Higgins, M.S., 1970. Longshore Currents Generated by Obliquely Incident Sea Waves, 1 and 2. <u>J. Geophysical Research</u>, 75(33), 6778-6801.

McDougal, W.G. and R.T. Hudspeth, 1981. Wave Induced Setup/Setdown and Longshore Current; Non-Planar Beaches: Sediment Transport. <u>Oceans</u>, IEEE, 834-846.

McDougal, W.G. and R.T. Hudspeth, 1984. Longshore Sediment Transport on Dean Beach Profiles. <u>Proc., 19th Int. Conf. on Coastal</u> <u>Eng.</u>, ASCE, 1488-1506.

Sawaragi, T. and I. Deguchi, 1978. Distribution of Sand Transport Rate Across a Surf Zone. <u>Proc., 16th Int. Conf. on Coastal</u> <u>Eng.</u>, ASCE, 1596-1613.

Sternberg, R.W., N.C. Shi and J.P. Downing, 1984. Field Investigations of Suspended Sediment Transport in the Nearshore Zone. <u>Proc., 19th Int. Conf. on Coastal Eng.</u>, ASCE, 1782-1798.